

Continuous and correlated nucleation during nonstandard island growth at Ag/Si(111)-7×7 heteroepitaxy

P. Kocán, P. Sobotík,* and I. Ošťádal

Department of Electronics and Vacuum Physics, Faculty of Mathematics and Physics, Charles University, V Holešovičkách 2, 180 00 Praha 8, Czech Republic

M. Kotrla

Institute of Physics, Academy of Sciences of the Czech Republic, Na Slovance 2, 182 21 Praha 8, Czech Republic

(Received 1 September 2003; revised manuscript received 23 December 2003; published 20 April 2004)

We present a combined experimental and theoretical study of submonolayer heteroepitaxial growth of Ag on Si(111)-7×7 at temperatures from 420 K to 550 K when Ag atoms can easily diffuse on the surface and the reconstruction 7×7 remains stable. Scanning tunneling microscopy measurements for coverages from 0.05 ML to 0.6 ML (ML—monolayer) show that there is an excess of smallest islands (each of them fills up just one half unit cell—HUC) in all stages of growth. Formation of a two-dimensional (2D) wetting layer proceeds by continuous nucleation of the smallest islands in the proximity of larger 2D islands (extended over several HUC's) and following coalescence with them. Such a growth scenario is verified by kinetic Monte Carlo simulation which uses a coarse-grained model based on a limited capacity of HUC and a mechanism which increases nucleation probability in a neighborhood of already saturated HUC's (correlated nucleation). The model provides a good fit for experimental dependences of the relative number of Ag-occupied HUC's and the preference in occupation of faulted HUC's on temperature and amount of deposited Ag. Parameters obtained for the hopping of Ag adatoms between HUC's agree with those reported earlier for initial stages of growth. The model provides two parameters—maximum number of Ag atoms inside HUC, and on HUC boundary.

DOI: 10.1103/PhysRevB.69.165409

PACS number(s): 68.55.Ac, 81.15.Kk, 81.15.Aa, 68.37.Ef

I. INTRODUCTION

Heteroepitaxial growth of metals on silicon surfaces has been studied for decades and morphologies of various grown structures were reported.^{1–6} Reconstruction of oriented semiconductor surfaces determines the mobility of deposited adatoms and substantially influences growth mechanism. Recently reported experimental studies on self-organized growth of arrays of ordered metal islands—quantum dots—on the Si(111)-7×7 surface^{4,7} stimulate need of detailed understanding of mechanisms controlling the growth. Heteroepitaxy of Ag on the Si(111)-7×7 surface represents one of frequently studied problems due to nonreactivity of Ag with the reconstructed surface, abrupt interface, and negligible interdiffusion of both elements. The growth mode is of the Stranski-Krastanov-type—three-dimensional (3D) islands are formed on a 2D Ag transition layer (wetting layer) grown on the 7×7 silicon surface.

Our initial scanning tunneling microscopy (STM) study of Ag/Si heteroepitaxy at low coverage⁵ showed a growth mechanism affected by trapping Ag adatoms in triangular units of the 7×7 reconstruction—half unit cells (HUC's). The HUC's are of two types: “faulted,” FHUC (containing a structural fault according to the dimer-adatom-stacking fault model⁸) and “unfaulted,” UHUC. For deposited Ag atoms, the two types of HUC's represent potential wells with different depths $E_F > E_U$. This leads to preferential nucleation in the FHUC's (the preference P_F is defined as a ratio of FHUC's containing Ag adatoms to all occupied HUC's). In the successive work⁹ we investigated processes of adatom diffusion, nucleation and island formation at the beginning of

the Ag growth for a deposited amount < 0.1 ML (ML—Monolayer) ($1 \text{ ML} \approx 7.83 \times 10^{14} \text{ atoms/cm}^2$), both experimentally and theoretically. We developed and used a simple coarse-grained model for the kinetic Monte Carlo (KMC) simulations. Fitting of experimental data provided values $E_F \approx E_U = (0.75 \pm 0.10) \text{ eV}$, $E_F - E_U < 0.05 \text{ eV}$, and frequency prefactors $\nu_F^0 \approx \nu_U^0 = 5 \times 10^{(9 \pm 1)} \text{ s}^{-1}$.

Recently, we extended our STM measurements to coverages up to 0.6 ML.⁶ In this regime a discontinuous 2D film, wetting layer,¹⁰ is formed. We observed large 2D islands completely covering several HUC's. We did not observe any island to overgrow the HUC boundaries at its perimeter. This results in triangularly jagged island shapes. There was a considerable number of stable Ag clusters—each of them formed *inside* a HUC. We denoted such islands as 1-HUC islands. These islands were observed for coverages up to 0.6 ML and for high temperatures (540 K) as well. Statistical analysis of island population on the surface revealed a number of 1-HUC islands much higher than a value expected by the “standard” model of island film growth¹¹ in which island density saturates and then all adatoms are captured by existing islands.

We suggested a possible growth mechanism compatible with our observations: A single 1-HUC island grows by adatom capturing until a maximum number of adatoms which can be accommodated in a HUC is reached—a 1-HUC island is saturated. The saturated and isolated island does not capture diffusing adatoms anymore. It leads to an increase of Ag adatom concentration around such islands and results in enhanced nucleation of new islands in proximity of saturated HUC's (correlated nucleation). Larger islands grow by coa-

lescence of smaller saturated islands.

In this paper, we verify the above nonstandard growth scenario by a combined experimental and theoretical study. We performed STM experiments in a temperature range when Ag atoms can easily diffuse on the surface and the structure 7×7 remains stable. We measured dependences of several structure related quantities (object densities, preferences of occupation, island size distribution) on deposited amount, substrate temperature and deposition flux. We show that the results of measurements can be explained by KMC simulation using a modified coarse-grained model developed from the one we used for low coverage growth.⁹ The new model, which takes into account limited capacity of HUC's and correlated nucleation, explains both morphological and statistical properties of island growth and coalescence on the reconstructed Si(111)- 7×7 surface.

II. EXPERIMENTS

Series of samples with various amounts of deposited Ag from 0.05 ML to 0.6 ML were prepared at temperatures from 420 K to 550 K at deposition rate $F_1=0.011$ ML s^{-1} . Another series with Ag amounts from 0.05 ML to 0.3 ML were deposited at $T=(492\pm 10)$ K and deposition rate $F_2=0.0005$ ML s^{-1} . Ag was evaporated from a tungsten filament in an ultrahigh vacuum chamber, the deposited amount was measured by a quartz thickness monitor with an absolute accuracy of $\pm 10\%$. Sb doped Si(111) substrates with a miscut of $\pm 0.1^\circ$ and resistivity of 0.005–0.01 Ω cm were heated by passing dc current (temperature calibrated with accuracy of ± 10 K). Other experimental details (substrate treatment, thickness monitor, and temperature calibration, etc.) have been already reported elsewhere.^{9,12} Before STM measurements, deposited films relaxed at least 1 h at room temperature (RT). Experimental procedures were performed at pressure $< 2\times 10^{-8}$ Pa. We used a STM of our design and construction with electrochemically polished tungsten tips.

III. EXPERIMENTAL RESULTS

Figure 1(a) shows an example of morphology of Ag islands grown at substrate temperature 490 K as observed in STM. Following morphological features have been found by analysis of a large number of images taken from various samples.

(i) Ag forms 2D islands of various sizes bordered always by dimer rows of the 7×7 reconstruction. The dimer rows at island boundary are not filled by Ag atoms, dimer rows inside larger islands are filled (overgrown) by Ag atoms—see detail A on Fig. 1(b).

(ii) We often observed islands covering adjacent HUC's but clearly separated by the dimer row—see detail B in Fig. 1(b).

(iii) Triangular shapes of larger islands follow the orientation of FHUC's [see Fig. 1(a) and Ref. 6].

(iv) An important feature is excess of 1-HUC islands in island size distribution even at very low deposition rates, higher temperatures, and coverages up to 0.6 ML.¹³ This is

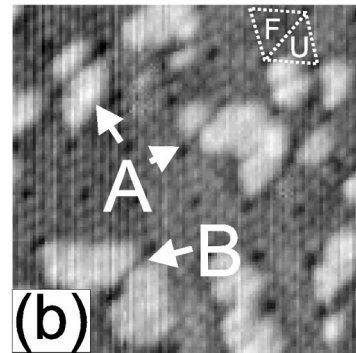
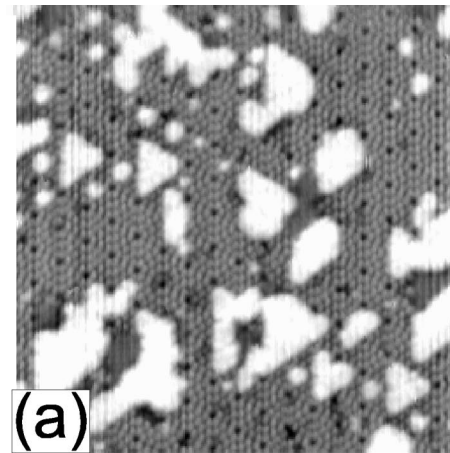


FIG. 1. (a) STM image of island morphology—white objects are Ag islands, with the exception of the smallest dots (impurities), 35×35 nm² area, evaporated amount $d=(0.5\pm 0.1)$ ML at temperature $T=490$ K and flux $F=0.0005$ ML s^{-1} . (b) Detail of island morphology, 16×16 nm² area: A, the 1-HUC island grown in a HUC adjacent to a larger island; B, two larger separated islands.

illustrated in Fig. 2 which shows the island size distribution for different coverages (see also Fig. 1 and Fig. 2 in Ref. 6). The basic size unit is an area of one HUC. The 1-HUC islands clearly dominate in all distributions.

The 1-HUC islands grow preferentially in FHUC's and in proximity of larger islands rather than in vacant areas of the

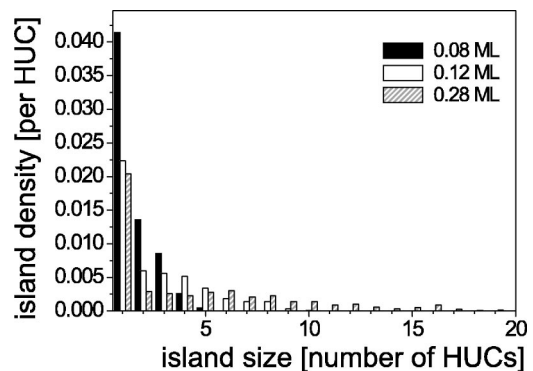


FIG. 2. Island size distribution for three different coverages. Samples were prepared at temperature 490 K and at deposition rate 0.011 ML s^{-1} .

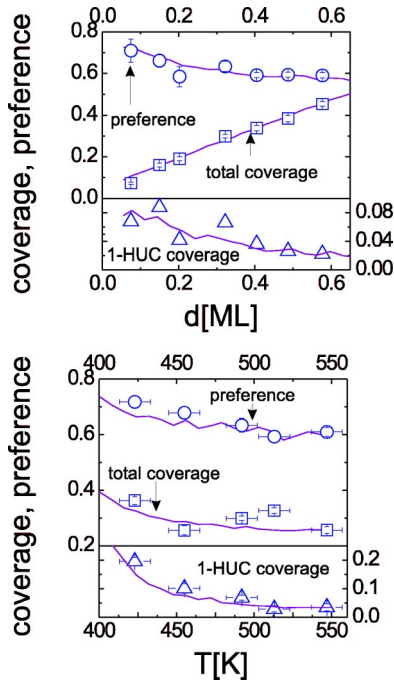


FIG. 3. Dependence of total coverage, 1-HUC coverage, and preference on amount of deposited Ag at $T=490$ K (upper panel) and on substrate temperature for $d=0.3$ ML (lower panel). Symbols—experimental data, lines—best fit using the model with center and boundary areas. All samples were prepared at deposition rate $F_1=0.011$ ML s^{-1} .

surface [Fig. 1(a)]. The formation of the wetting layer proceeds as continuous nucleation of new 1-HUC islands.

(v) STM imaging at room temperature does not allow to distinguish number of Ag atoms contained in the 2D Ag island¹⁴ with exception of the smallest objects—HUC's containing one or two atoms.

The following quantities were obtained by statistical analysis of STM images: preference P_F , island size distribution (island size is measured in numbers of HUC's covered by the island), total coverage θ —the relative number of occupied HUC's (ratio of the occupied HUC's to the all HUC's on the surface), and 1-HUC coverage $\theta_{1\text{-HUC}}$ —the relative number of 1-HUC islands (defined similarly). Ag objects are nonempty HUC's as well as islands larger than a HUC. When no Ag islands larger than a HUC are present $\theta = n_{\text{Ag}}$, where n_{Ag} is density of Ag objects (number of objects normalized to the number of all HUC's on the surface). The preference P_F reflects existence of two different potential wells $E_F > E_U$ on the surface.

We measured dependences of P_F , θ and $\theta_{1\text{-HUC}}$ on deposited amount d (upper panel in Fig. 3) and substrate temperature (lower panel in Fig. 3). In the studied range of deposition parameters the total coverage θ is proportional to the deposited amount of Ag and decreases only slightly with the increasing substrate temperature. When islands larger than 1-HUC begin to grow, preference P_F decreases with both the deposited amount and the substrate temperature. However, it remains larger than 0.6 due to continuous nucleation of new 1-HUC islands preferably in FHUC's.

IV. SIMULATION MODELS

A. Original model

A coarse-grained KMC model with an algorithm derived from Ref. 15 was successfully applied for simulation of early stages of nucleation.⁹ The model uses HUC's as basic units of the surface. Events included in the model correspond to the following growth scenario: Ag atoms arrive at the surface in random positions with a rate given by flux F . Diffusion of Ag adatoms on the Si substrate is modeled by thermally activated hops to neighboring HUC's. Depending on the HUC type, there are two different contributions to activation energy from interaction with the substrate. A frequency prefactor ν_0 is assumed (for simplicity) to be the same for FHUC's and UHUC's. The transient mobility of impinging Ag adatoms was included into the model to explain and simulate the short-range ordering of Ag objects and the low value of the total coverage at temperatures too low for sufficient adatom mobility between HUC's (Refs. 16 and 17) (however, in a temperature range, when Ag atoms can easily diffuse on the surface, this mechanism is not much important for the grown morphologies). Hopping adatoms can create nuclei inside HUC's. Let n be a number of Ag atoms in a HUC. The model assumes existence of a critical nucleus size n^* . Nuclei of more than n^* Ag atoms are stable. Nuclei with the size $n \leq n^*$ can decay with activation energy proportional to n . Hopping rate of an Ag atom out of a HUC is approximated as $\nu_n^{F,U} = n \nu_0 \exp\{-[E_{F,U} + (n-1)E_a]/k_B T\}$, where E_a represents effective Ag-Ag interaction and k_B is Boltzmann's constant. The values $E_F \approx E_U = (0.75 \pm 0.10)$ eV, $E_F - E_U < 0.05$ eV, $E_a \approx 0.05$ eV, critical nucleus size $n^* = 5$, and the frequency prefactor for hopping out of HUC's, $\nu_0 = 5 \times 10^{(9 \pm 1)} s^{-1}$, were obtained in the Ref. 9. The original model has been used only for low coverages where real limits of capacity of HUC's cannot be reached. HUC's were treated like potential wells with unlimited capacity. When higher amount of Ag is deposited this simplification has to be replaced by a certain restriction.

B. Model with a simple constraint

The simplest way how to introduce a limitation of capacity is its direct implementation within a "standard" growth scenario¹¹ for growth simulations. At the beginning of growth the density of Ag nuclei reaches a saturated value and the islands grow simply by capturing hopping adatoms. Each HUC can accommodate n_H Ag atoms at the most and the next deposited or diffusing atom is forced to sit to the nearest HUC occupied by less than n_H Ag atoms. Hence, an island containing more than n_H adatoms overgrows HUC boundaries and extends over neighboring HUC's.

We tried to fit experimental data using the above simple modification. The same model and parameter values as in Ref. 9 were used, only limited capacity of a HUC, n_H , was included. The value n_H was determined by fitting the experimentally obtained dependence of the relative number of occupied HUC's, θ , on deposited amount d . The fit provided the value of $n_H = 45 \pm 5$. However, the morphology obtained by using "standard" mechanism differs from the experimen-

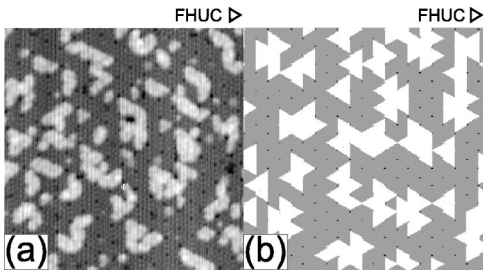


FIG. 4. (a) STM image of $35 \times 35 \text{ nm}^2$ area, deposited amount $d = (0.50 \pm 0.05) \text{ ML}$ at temperature $T = 490 \text{ K}$ and flux $F = 0.011 \text{ ML s}^{-1}$; (b) layer simulated under the same conditions using “standard” 2D growth scenario (model with a simple constraint).

tal data, Fig. 4. Only a few 1-HUC islands are visible in the simulated layer. A statistical analysis of the experimental results reveals excess of 1-HUC islands in comparison with the simulated growth, Fig. 5. Therefore, the concept of limited capacity needs to be implemented in a more subtle way taking into account the role of 1-HUC islands in agreement with the scenario suggested in Ref. 6 and detailed experimental observations presented in Sec. III.

C. Model with center and boundary areas—final model

During the growth a 1-HUC island captures more and more diffusing adatoms until its size reaches a saturated value n_S given by the limited capacity of the HUC. The saturated 1-HUC Ag island cannot further grow by adatom capture. The value n_S is assumed to be the same for islands in both types of HUC's. When a diffusing adatom meets the saturated HUC, it hops fast out leaving dimer row unoccupied. This event is simulated by means of setting the energy barrier for hopping out of saturated HUC's close to zero value.

Larger islands grow by coalescence with 1-HUC islands only by the following mechanism: Boundaries between adjacent HUC's can be filled only if the cells are saturated. Such two HUC's can coalesce with assistance of a certain number of hopping adatoms, n_B , completing each HUC. In the simulation, the adjacent saturated HUC's can incorporate new adatoms until the boundary areas in HUC's (dimer rows

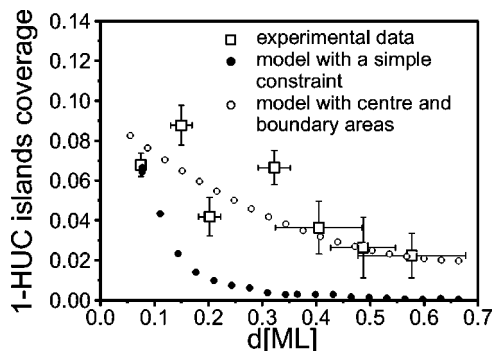


FIG. 5. Comparison of the dependence of 1-HUC island coverage on deposited amount at temperature $T = 490 \text{ K}$ and flux $F = 0.011 \text{ ML s}^{-1}$ in experiment and in two different models.

separating adjacent HUC's) are filled by Ag atoms. The maximum number of atoms in a HUC with all the boundary areas filled is then $n_S + 3 \times n_B$. Therefore, in the computer model, each HUC is formally divided into one center and three boundary areas. The boundary area can accept Ag atoms if the center areas of both adjacent HUC's are saturated—each contains n_S Ag atoms (i.e., a saturated 1-HUC island).

Each hopping event in the computer model is selected with probability determined by activation energy calculated with respect to a number of Ag atoms at a given position (HUC). We started with simulations in which the hopping probability was not affected by occupancy of a destination site (HUC). These simulations provided high population of 1-HUC islands but fitting of model parameters failed in achieving quantitative agreement with the experimentally measured dependences. The concentration of 1-HUC islands obtained by the simulations was much higher than the experimentally observed value. The experimentally observed increase of 1-HUC island density in proximity of larger islands was not reproduced by the model.

The enhanced nucleation of a new island in proximity of the saturated one (in an adjacent HUC) can be explained physically by an increase of time spent by a diffusing Ag adatom in the close neighborhood of saturated HUC. This might be caused by an interaction of Ag adatom with Ag atoms in saturated HUC. Another reason may be a change of the barrier for diffusion over the boundary of saturated HUC due to relaxation of Si atoms. The effect is modeled by decrease of the barrier for hopping into the saturated HUC by ΔE_S . It increases probability of nucleation near the saturated island. The correlated nucleation would also imply decrease of the concentration of 1-HUC islands because during further growth more 1-HUC islands will join larger islands. This modification implies the need to use a model with hopping rates depending on a final position. The introduction of anisotropy for hopping makes the code technically a bit more complicated (a hop-oriented code has to be employed).

V. SIMULATION RESULTS AND DISCUSSION

Simulations with the final model (the model with center and boundary areas) reproduce well growth morphologies observed in the experiment. Figures 6(a) and 6(b) show examples of real and simulated growth morphologies for two temperatures $T = 490 \text{ K}$, $T = 550 \text{ K}$ and for the rate of deposition $F_1 = 0.011 \text{ ML s}^{-1}$. Comparison of corresponding figures shows that an excess of 1-HUC islands is well reproduced for both temperatures.

We carefully fitted the experimental data presented in Fig. 3. To simplify the fitting, we assumed $n^* = 5$ and $E_d = 0.05 \text{ eV}$ as obtained in the previous work.⁹ We varied three parameters n_S , n_B , and ΔE_S and at the same time we were changing values E_F and E_U within error bars of the previous work to find the best fit.

We found that the fitting of experimental data using the final model gives values $\nu_0 = (5 \times 10^9 \pm 1) \text{ s}^{-1}$ and $E_F \approx E_U = (0.68 \pm 0.10) \text{ eV}$ (at the fixed value $\nu_0 = 5 \times 10^9 \text{ s}^{-1}$ the values E_F, E_U can be determined with an accuracy of 0.02

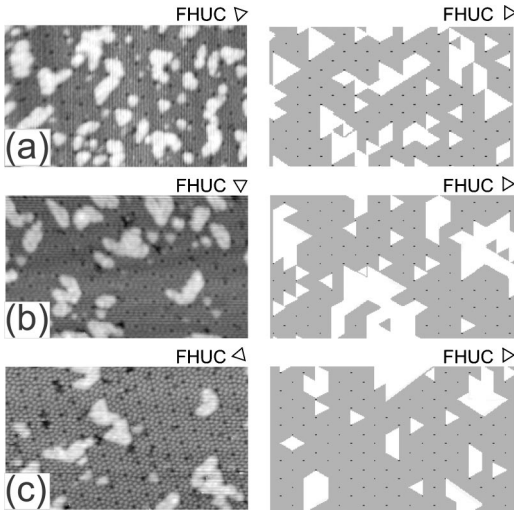


FIG. 6. Examples of experimental (left column) and simulated (right column) morphology of films with $d=(0.32\pm 0.03)$ ML obtained by deposition at two temperatures and two deposition rates (a) $T=490$ K, $F_1=0.011$ ML s^{-1} ; (b) $T=550$ K, $F_1=0.011$ ML s^{-1} ; (c) $T=490$ K, $F_2=0.0005$ ML s^{-1} . Area 35×20 nm 2 . The model with center and boundary areas was used.

eV) and the difference $E_F-E_U=(0.03\pm 0.01)$ eV. The values are in a good agreement with our previous results.⁹ In addition the model provided energy related to effective interaction with saturated HUC, $\Delta E_S=(0.10\pm 0.05)$ eV, and numbers of Ag atoms $n_S=21\pm 6$, and $n_B=5\pm 2$. Maximum number of Ag atoms accommodated in a HUC with all three boundary areas filled is 36 ± 8 . It is larger than a rough estimate reported in Ref. 6 (compare also with a value of 45 ± 5 resulted from the “standard” growth model). The value of n_S is consistent with a number of potential minima in a HUC—18—proposed in Ref. 18.

The validity of the final model and the values of the parameters were further tested for quite different growth condition, very low deposition rate $F_2=0.0005$ ML s^{-1} . STM image in left part of Fig. 6(c) shows that there is excess of 1-HUC’s even in this regime. Morphology obtained by simulation under the same growth conditions in right part of Fig. 6(c) has similar features. A series of samples provided dependences [see Fig. 7(a)] similar to those shown in Fig. 3. In the same figure, we show results obtained by calculation using the final model with the parameters given above. There was no additional fitting. We can see that the agreement is quite good. The model explains well excess of 1-HUC islands in the size distribution also for this much lower deposition rate—see a reasonable agreement between experimental data and simulation [Fig. 7(b)].

STM images of layers grown at various conditions show that a mean size of large irregular Ag islands is limited. During further growth the islands connect into a network—the wetting layer. The morphology of the irregular islands and wetting layer depend on growth temperature^{6,10} and are driven by epitaxial strain. The current model does not take into account the strain which plays an important role in the formation of wetting layer. Therefore, the model cannot be used for simulation of growth above 0.6 ML of deposited

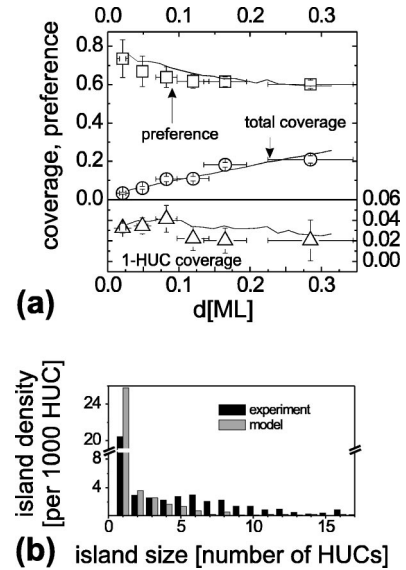


FIG. 7. Comparison of experimental (symbols) and simulated (lines—best fit using the model with center and boundary areas) data for films prepared at low deposition rate $F_2=0.0005$ ML s^{-1} at temperature $T=490$ K. (a) dependence of coverages and preference on deposited amount, (b) island size distribution.

metal but it allows to assess the structural properties of filling individual HUC’s.

VI. CONCLUSIONS

Combined study of submonolayer growth of Ag on Si(111)-(7 \times 7) by series of STM measurements and kinetic Monte Carlo simulations allowed to determine microscopic mechanism of growth in the regime of island coalescence. The surface reconstruction strongly affects nucleation and growth of islands. Islands do not extend laterally but by fast connection of preformed blocks—saturated HUC’s—by filling dimer rows. Key feature of growth is slow and *continuous* nucleation of new small nuclei occupying the inner parts of HUC preferably in proximity of already saturated HUC’s.

Both surface morphologies and quantitative measurements can be reproduced by KMC simulations using a model extending the coarse-grained model utilized for simulation of initial stages of growth. It turned out that it was necessary to resolve the inner part of HUC and its boundary. Comparison with experiment confirmed the applicability of this model for interpretation of growth for a large range of deposition parameters (temperature, deposition rate, time) and for deposited amount up to 0.6 ML. Correlated nucleation in proximity of saturated HUC’s is obtained by introduction of effective interaction *decreasing* energy barrier for a hop into the saturated HUC by $\Delta E_S=(0.10\pm 0.05)$ eV. The model can be used for simulations up to the coverage when epitaxial strain significantly influences growth of larger islands.

The model allowed to assess maximum numbers of Ag atoms per HUC in a 2D island: for an isolated 1-HUC island $n_S=21\pm 6$; for a larger island (covering ≥ 2 HUC’s) the saturated number of Ag atoms filling one of the three boundary areas is $n_B=5\pm 2$ and the maximum number of Ag at

oms per HUC is 36 ± 8 ($n_S + 3 \times n_B$).

We expect that the mechanism of growth on reconstructed Si(111)-(7×7) for other nonreactive metals is similar and that the model can be used as a starting point for modeling heteroepitaxial growth in other systems and for fitting corresponding parameters.

ACKNOWLEDGMENTS

This work was supported by the Grant Agency of the Czech Republic, Project No. 202/01/0928, and by the Ministry of Education, Youth and Sports of Czech Republic, Project No. FRVŠ 2735/2003.

*Electronic address: Pavel.Sobotik@mff.cuni.cz

¹Y. Tanishiro, K. Kaneko, H. Minoda, K. Yagi, T. Sueyoshi, T. Sato, and M. Iwatsuki, *Surf. Sci.* **358**, 407 (1996).

²O. Custance, I. Brihuega, J.-Y. Veuillen, J. Gomez-Rodriguez, and A. Baro, *Surf. Sci.* **482–485**, 878 (2001).

³S. Tosch and H. Neddermeyer, *Phys. Rev. Lett.* **61**, 349 (1988).

⁴L. Vitali, M.G. Ramsey, and F.P. Netzer, *Phys. Rev. Lett.* **83**, 316 (1999).

⁵P. Sobotík, I. Ošt'ádal, J. Mysliveček, and T. Jarolímek, *Surf. Sci.* **454–456**, 847 (2000).

⁶P. Sobotík, I. Ošt'ádal, and P. Kocán, *Surf. Sci.* **507–510**, 389 (2002).

⁷J.-L. Li, J.-F. Jia, X.-J. Liang, X. Liu, J.-Z. Wang, Q.-K. Xue, Z.-Q. Li, J.S. Tse, Z. Zhang, and S.B. Zhang, *Phys. Rev. Lett.* **88**, 066101 (2002).

⁸K. Takayanagi, Y. Tanishiro, and S. Takahashi, *J. Vac. Sci. Technol. A* **3** (3), 1502 (1985).

⁹J. Mysliveček, P. Sobotík, I. Ošt'ádal, T. Jarolímek, and P. Šmilauer, *Phys. Rev. B* **63**, 045403 (2001).

¹⁰P. Sobotík, I. Ošt'ádal, T. Jarolímek, and F. Lavický, *Surf. Sci.* **797**, 482 (2001).

¹¹J.A. Venables, *Rep. Prog. Phys.* **47**, 399 (1984).

¹²J. Mysliveček, Ph.D. thesis, Charles University, Prague, 2000.

¹³We do not observe any clean evidence of selection of magic island sizes as in the case of Si growth on Si(100), see. B. Voigtländer, M. Kästner, and P. Šmilauer, *Phys. Rev. Lett.* **81**, 858 (1998).

¹⁴T. Jarolímek, J. Mysliveček, P. Sobotík, and I. Ošt'ádal, *Surf. Sci.* **482**, 386 (2001).

¹⁵S. Clarke, M.R. Wilby, and D.D. Vvedensky, *Surf. Sci.* **225**, 91 (1991).

¹⁶To explain this, an alternative mechanism of correlated diffusion 17 was suggested. Both mechanisms can give in principle satisfactory results. Only further experimental data together with the theoretical effort can clarify this issue.

¹⁷E. Vasco, C. Polop, and E. Rodríguez-Cañas, *Phys. Rev. B* **67**, 235412 (2003).

¹⁸K. Cho and E. Kaxiras, *Europhys. Lett.* **39**, 287 (1997).